KEK-TH-741
CERN-TH/2001-022
YITP-01-04
hep-ph/yymmdd
February 7, 2001

The fate of the B ball

Junji Hisano[a,b], Mihoko M. Nojiri[c] and Nobuchika Okada[a]

(a) Theory Group, KEK, Oho 1-1, Tsukuba, Ibaraki 305-0801, Japan

(b) Theory Devision, CERN, 1211 Geneva 23, Switzerland

(c) YITP, Kyoto University, Kyoto 606-8502, Japan

Abstract

The gauge-mediated SUSY-breaking (GMSB) model needs entropy production at a relatively low temperature in the thermal history of the Universe for the unwanted relics to be diluted. This requires a mechanism for the baryogenesis after the entropy production, and the Affleck and Dine (AD) mechanism is a promising candidate for it. The AD baryogenesis in the GMSB model predicts the existence of the baryonic Q ball, that is the B ball, and this may work as the dark matter in the Universe. In this article, we discuss the stability of the B ball in th presence of baryon-number violating interactions. We find that the evaporation rate increases monotonically with the B-ball charge because the large field value inside the B ball enhances the effect of the baryon-number-violating operators. While there are some difficulties to evaluate the evaporation rate of the B ball, we derive the evaporation time (lifetime) of the B ball for the mass-to-charge ratio $\omega_0 \gtrsim 100$ MeV. The lifetime of the B ball and the distortion of the cosmic ray positron flux and the cosmic background radiation from the B ball evaporation give constraints on the baryon number of the B ball and the interaction, if the B ball is the dark matter. We also discuss some unresolved properties of the B ball.

1 Introduction

The gauge-mediated SUSY-breaking (GMSB) model [1] is one of the complete models to solve the FCNC problem in the supersymmetric (SUSY) extension of the Standard Model (SM). In a typical GMSB model [2], the dynamical SUSY-breaking scale is of the order of 10^7 GeV, so that the SUSY-breaking masses of the order of the weak scale (m) are generated in the SUSY SM. This predicts a gravitino with a mass $m_{3/2} = 100$ keV, which is beyond the closure limit of the Universe, $m_{3/2} < 2h^2$ keV [3]. It is very unlikely that such a small gravitino mass can be generated in the GMSB model, while there is an exceptional extension for it [4]. Also, the string moduli may supply another problem in cosmology, since it is expected to have a mass of the order of $m_{3/2}$.

This implies that there must be a substantial entropy production in such a way that they can be diluted in the thermal history of the Universe, we therefore have to consider a possible mechanism of baryogenesis at a relatively low temperature. A promising candidate for it is the Affleck and Dine (AD) mechanism [5][6]. One of the important predictions of the AD baryogenesis in the GMSB model is the existence of *a stable Q ball* [7]. It can be a candidate for the dark matter (DM) in the Universe.

The Q ball, a non-topological soliton, is a coherent state of a complex scalar field [8]. The existence and the stability come from a global U(1) quantum number. In the SUSY SM the Q ball is composed of squarks and/or sleptons with baryon (B) or lepton (L) numbers [9]. In the GMSB model, the flat directions ϕ composed of the squarks and/or sleptons are lifted up by at most a logarithmic potential for the large field value due to the SUSY breaking [6]. This leads to the existence of the stable Q ball. The mass of the Q ball originated from the flat direction is proportional to $\mathbf{m}Q^{\frac{3}{4}}$, not to mQ, because of the logarithmic potential. Here, $\mathbf{m}$ is the mass scale of a logarithmic potential ($\mathbf{m} \simeq 10^{3-5}$ GeV). Therefore, the baryonic Q ball, the B ball, may be stable against the decay into nucleons if the baryon number is sufficiently large ($Q \gtrsim 10^{12}$), since the mass-to-charge ratio ω_0 can become less than 1 GeV.

The AD baryogenesis, which is the natural candidate for baryogenesis in the GMSB model, as mentioned above, can generate such large B balls. In the final stage of the AD baryogenesis, the coherent state of the AD scalar field, which consists of the flat direction ϕ, becomes unstable and instabilities develop. The Q ball is formed as a result of the fluctuation glowing. This behaviour of the AD field has been justified by numerical simulations [10], and the largest Q ball charge is proportional to the initial field value of the AD field. Then, the B ball dark matter is an important prediction in the GMSB model, assuming the AD baryogenesis.

The B ball DM search has already given a constraint on this scenario. Since the B ball with larger baryon number becomes stabler, the B ball absorbs nucleons and emits an energy of about 1 GeV per a nucleon when the B ball collides with nucleons. This process is known as the KKST process, and it is similar to the monopole-catalyzed proton decay [11]. From the BAKSAN, Gyrlyanda, and Kamiokande experimental results, the constraint on the B ball charge is derived assuming that the B ball is the DM, and it should be larger than 10^{24} for $\mathbf{m} < 1$ TeV [12]. This KKST process is suppressed by the Coulomb repulsion if the B ball has positive electric charge. The B ball has an electron cloud around it and behaves as a heavy atom. The interaction with matter is similar to the case of nuclearites and the B ball charge should be larger than 10^{22-30}, depending on the electric charge [12].

These bounds are loosened if the supergravity contribution to the flat direction potential is included [13]. For a large B ball charge, the field value inside the B ball becomes large and the supergravity contribution to the flat direction potential is not negligible. In this case, for a larger B ball, its radius R_Q does not increase and becomes a constant, $\sim 10/m_{3/2}$. The geometrical cross section πR_Q^2 is smaller than when the supergravity contribution is not included.

In this article we derive another constraint on the B ball DM scenario. The baryon number may not be an exact symmetry in nature, and high-energy physics may violate the baryon-number conservation, such as in the grand unified theories (GUTs). In fact, the AD baryogenesis needs the $(B-L)$-violating operators, which kick ϕ to start the rotation and to generate the baryon number. While the interaction with only lepton-number violation can work for the AD baryogenesis, the baryon-number-violating operators are needed to generate for the B ball to be generated in the AD mechanism. In this article, assuming the existence of the baryon-number-violating higher-dimensional operators, we evaluate the lifetime (the evaporation rate) of the B ball. The higher-dimensional operators, including ϕ, enhance the evaporation rate by the large field value inside the B ball. Especially, for a larger B ball, the field value becomes larger and the evaporation rate is significantly enhanced. As a result, the B ball does not necessarily keep the baryon number beyond the age of Universe.

The final state in the evaporation of the B ball by the baryon-number-violating operators depends on the quantum numbers of the B ball, the symmetries of the operators, and ω_0. If the operator violates $(B+L)$, but not $(B-L)$, and the B ball does not have lepton numbers at all, the final states are (e^+, π^-), $(\bar{\nu}, \pi^0)$, and so on for $\omega_0 \gtrsim 100$ MeV. If $\omega_0 \lesssim 100$ MeV, the final state consists of only lepton and antileptons. Photons may be included there. Without the knowledge about the surface dynamics on the B ball, one cannot estimate the evaporation rate in the case $\omega_0 \lesssim 100$ MeV. Since the pion emission from the B ball is not allowed kinematically, quarks emitted by the baryon-number-violating operators are bounded to the surface or inside of the B ball for a while, and they decay or annihilate to the lighter particles. In this article, we restrict ourselves to evaluating the evaporation rate in the case $\omega_0 \gtrsim 100$ MeV; we discuss what may happen for $\omega_0 \lesssim 100$ MeV.

If e^+ is in the final state, the energy is of the order of ω_0 and almost monochromatic. This may change the cosmic ray positron flux. The existing positron flux measurements are above about 100 MeV, which works for our case of $\omega_0 \gtrsim 100$ MeV. Also, when π^0 is in the final state, it may distort the cosmic background radiation. We find that both observations give more stringent constraints on the evaporation rate of the B ball than a comparison with the age of the Universe, assuming that the B ball is the DM.

We organize this article as follows. In the next section, we introduce the Q ball following Coleman's argument, and review the profile and the quantum numbers of the B ball originated from the flat directions of the squarks and/or sleptons in the GMSB model. Also, we show the profile of the Q ball configuration after including the supergravity contribution to the scalar potential. In Section 3, the final state of the B ball evaporation by the baryon-number-violating operators is discussed there for both $\omega_0 \gtrsim 100$ MeV and $\omega_0 \lesssim 100$ MeV. In Section 4, the evaporation rate of the B ball is presented for $\omega_0 \gtrsim 100$ MeV and it is compared with the age of the Universe. In Section 5, we evaluate the fluxes of the e^+ and γ emitted from the evaporation of the B ball, and give constraints on the evaporation rate from the observations. Section 6 is devoted to conclusions and discussion.

2 Properties of the B ball in the GMSB model

In this section we review the Q ball in order to fix our convention, and summarize the properties and the profiles of the B ball in the GMSB model. As Coleman pointed out [8], some scalar potential with a $\mathrm{U}_Q(1)$ symmetry predicts the Q ball to be a non-topological soliton. The Lagrangian of the scalar field with the $U_Q(1)$ charge q is

$$\mathcal{L} = |\partial_\mu \phi|^2 - V(\phi). \tag{1}$$

This system has two conserved quantities, the charge Q and the energy E,

$$Q = i \int d^3x \, q \left(\phi^\star (\partial_t \phi) - (\partial_t \phi^\star) \phi \right), \tag{2}$$

$$E = \int d^3x \left(|\partial_t \phi|^2 + |\partial_i \phi|^2 + V(\phi) \right). \tag{3}$$

In this system, the non-trivial lowest-energy state with Q fixed, that is the Q ball, is derived by minimizing

$$E_\omega = E + \omega \left\{ Q - i \int d^3x q \left(\phi^\star (\partial_t \phi) - (\partial_t \phi^\star) \phi \right) \right\}. \tag{4}$$

Here, ω is the Lagrange multiplier. The time dependence on ϕ of the Q ball configuration is determined as

$$\phi(x) = \tilde{\phi}(\boldsymbol{x}) \mathrm{e}^{-iq\omega t}, \tag{5}$$

and E_ω is reduced to be

$$E_\omega = \int d^3x \left((\partial_i \tilde{\phi})^2 + V_\omega(\tilde{\phi}) \right) + \omega Q, \tag{6}$$

where $V_\omega(\tilde{\phi}) = V(\tilde{\phi}) - q^2 \omega^2 \tilde{\phi}^2$. Then, the procedure to derive the Q ball configuration is by deriving a solution of $\tilde{\phi}$ for the equation of motion

$$\partial_r^2 \tilde{\phi} + \frac{2}{r} \partial_r \tilde{\phi} - \frac{1}{2} \frac{\partial V_\omega(\tilde{\phi})}{\partial \tilde{\phi}} = 0, \tag{7}$$

ϕ^n	B	L
$\bar{u}dd$	-1	0
$QQQL$	1	1
$\bar{u}\bar{u}d\bar{e}$	-1	-1
$QQQQ\bar{u}$	1	0
$dddLL$	-1	2
$\bar{u}\bar{u}\bar{u}\bar{e}\bar{e}$	-1	-2
$\bar{u}\bar{u}dddd$	-2	0
$QQQQdLL$	1	2
$QQQLLL\bar{e}$	1	2
$\bar{u}\bar{u}\bar{u}ddd\bar{e}$	-2	-1

Table 1: The renormalisable F and D flat directions in the SUSY SM with the baryon numbers. Q and L stand for the doublet quarks and leptons, and $\bar{u}$, $\bar{d}$, and $\bar{e}$ for singlet quarks and leptons.

with the boundary condition $\partial_r\tilde{\phi}(0) = \tilde{\phi}(\infty) = 0$, and minimizing E_ω for ω.

We now discuss the properties and the profiles of the B ball in the GMSB model. The large B ball originates from the flat direction ϕ consisting of squarks and/or sleptons in the GMSB model. A typical example of the renormalisable F and D flat directions is given as

$$\bar{u}_2^\alpha = \frac{1}{\sqrt{3}}\phi\delta_1^\alpha,\ \bar{d}_1^\alpha = \frac{1}{\sqrt{3}}\phi\delta_2^\alpha,\ \bar{d}_2^\alpha = \frac{1}{\sqrt{3}}\phi\delta_3^\alpha. \tag{8}$$

Here, $\bar{u}$ and $\bar{d}$ are singlet quarks, the upper and lower indices for colour and generation, respectively. The coefficients in the right-hand sides of Eqs. (8), $1/\sqrt{3}$, is for the canonical normalization of ϕ. The renormalizable F and D flat directions in the SUSY SM are summarized in Ref. [14]. Here, we present only the flat directions with the baryon numbers in Table 1. Here, Q and L stand for the doublet quarks and leptons, and $\bar{e}$ for singlet leptons. We suppressed the gauge and generation indices. The charge for the B ball composed of the flat direction follows the charge of this direction. This is important for determining the final states in the evaporation of the B ball.

Which type of the B ball listed in Table 1 is the DM in the Universe as the result of the AD mechanism? For a fixed baryon number Q, the stable B ball should be only the lightest among those of the above flat directions. Even if the AD mechanism creates heavier B balls with the same baryon number Q as the lightest one, they change their lepton numbers by emitting neutrinos and/or anti-neutrinos, and transit to the lightest one. However, the transition rate should be suppressed, and the transition time might be longer than the age of the Universe. This is because the potential barrier between the two states is very high due to the large field values. Therefore, we will not calculate the transition rate to the lightest state, however, discuss the evaporation of the B ball generically.

Next, we show the profiles of the B ball in the GMSB model. In that model the flat direction has a logarithmic potential due to the radiative correction from the messenger sector [6]. This implies that a larger B ball with a larger field value is energetically favoured for the unit charge, which leads to a stable B ball. In this article the scalar potential of the flat direction ϕ in the GMSB model is simplified as

$$V_{\rm GMSB} \;=\; \frac{(mM)^2}{2}\left(\log\left(1+\frac{|\phi|^2}{M^2}\right)\right)^2. \tag{9}$$

Here, m is the SUSY breaking scale in the SUSY SM ($m \sim O(10^{2-3})$ GeV), and M is for the messenger quark mass in the GMSB model. In a typical model, the messenger quark mass is of the order of 10^5GeV. While this double-log potential realizes the behaviour of the exact potential for $\phi \gg M$, derived in Ref. [6], it has a wrong behaviour for $\phi \ll M$. However, the Q ball properties are determined by the behaviour of the potential for $\phi \gg M$, and this potential thus works for our purposes.[1] The profile of the large B ball derived by this potential is well approximated to be

$$\tilde{\phi} \;=\; \tilde{\phi}_0 \frac{\sin(q\omega r)}{q\omega r}, \tag{10}$$

for $r < R_Q (\equiv \pi/q\omega)$, and $\tilde{\phi} = 0$, for $r \geq R_Q$. The parameters in Eq. (10) and the B ball mass determined from this profile are given by the B ball charge Q as

$$\begin{aligned} q\omega &= (2\pi\eta_0)^{\frac{1}{2}}(mM)^{\frac{1}{2}}(Q/q)^{-\frac{1}{4}}, \\ \tilde{\phi}_0 &= (\frac{\eta_0}{2\pi})^{\frac{1}{2}}(mM)^{\frac{1}{2}}(Q/q)^{\frac{1}{4}}, \end{aligned}$$

[1] In Ref. [7] they adopt a single-log potential and take $M = m$ in the potential so that the behaviour of the potential for $\phi \ll M$ is realized. We find that the field value inside the Q ball in our potential with $M = m$ is a few time larger than that in the single-log potential for a fixed Q.

$$
\begin{aligned}
R_Q &= \left(\frac{\pi}{2\eta_0}\right)^{\frac{1}{2}} (mM)^{-\frac{1}{2}} (Q/q)^{\frac{1}{4}}, \\
m_Q &= \frac{4}{3}(2\pi\eta_0)^{\frac{1}{2}}(mM)^{\frac{1}{2}}(Q/q)^{\frac{3}{4}}.
\end{aligned} \tag{11}
$$

In the following the flat directions are defined so that q, ω and ω_0 are positive. The parameter η_0 is fitted as

$$
\eta_0 \simeq 4.8 \log \frac{m}{q\omega} + 7.4. \tag{12}
$$

from the numerical calculation. For $r \gtrsim R_Q$, where $\tilde{\phi} \lesssim mM/q\omega$, the above approximated solution is not valid. However, such a region does not contribute dominantly to the properties of the B ball. In the following we call the B ball given by Eqs. (10) and (11) as the GMSB B ball.

From Eqs. (11), the energy per unit charge $\omega_0 (\equiv m_Q/Q)$ is

$$
\omega_0 = \frac{4}{3}\omega. \tag{13}
$$

The physical meaning of ω is the energy for increasing or decreasing the B ball charge by the unit charge, since $(m_Q - m_{Q-1}) = \omega$.

The field value $\tilde{\phi}_0$ is proportional to $Q^{\frac{1}{4}}$, as in Eq. (11), and for larger Q the supergravity contribution to the scalar potential may be important [13]. The scalar potential from the supergravity contribution is

$$
V_{\mathrm{SUGRA}} = m_{3/2}^2 |\phi|^2 \left(1 + K \log \frac{|\phi|^2}{M_G^2}\right), \tag{14}
$$

where $m_{3/2}$ is the gravitino mass and M_G is the reduced Planck mass. Here we assume the minimal supergravity for simplicity, and this potential becomes dominant when ϕ is larger than $mM/m_{3/2}$. The second term in the bracket of the right-hand side comes from one-loop correction. If it comes from the gauge interaction, K is negative and $O(10^{-2})$. The existence of the Q ball solution requires negative K [15]. In a limit where V_{GMSB} is negligible, the Q ball configuration is exactly given by a Gaussian form:

$$
\tilde{\phi} = \tilde{\phi}_0 \mathrm{e}^{-\frac{r^2}{2R_Q^2}}. \tag{15}
$$

This solution leads to

$$
\begin{aligned}
q\omega &= m_{3/2}, \\
\tilde{\phi}_0 &= (2\pi^{\frac{3}{2}})^{-\frac{1}{2}}|K|^{\frac{3}{4}} m_{3/2}(Q/q)^{\frac{1}{2}}, \\
R_Q &= |K|^{-\frac{1}{2}} m_{3/2}^{-1}, \\
m_Q &= m_{3/2}(Q/q),
\end{aligned}
\tag{16}
$$

up to $O(K)$ [15], and then

$$
\omega_0 = \omega. \tag{17}
$$

We refer to the B ball given by Eqs. (15) and (16) as the supergravity B ball.

In Fig. 1 we show the mass-to-charge ratio of the B ball, ω_0, as a function of Q. The solid line is for the B ball that comes from the flat-direction potential of the GMSB model (the GMSB B ball). The dashed lines are for those from the supergravity potential (the supergravity B ball). Here, we take $m = 1$ TeV, $M = 10^2$ TeV, and $q = 1/3$, assuming that the B ball comes from $\bar{u}\bar{d}\bar{d}$. If taking larger m or M, the solid line is shifted to the upper side. For smaller q, both the solid and dashed lines go up. In the region $\omega_0 > 1$ GeV, the B ball is unstable and decays into nucleons. While the result of the direct search for the B ball DM depends on the electric charge, the region for $Q \lesssim 10^{22}$ is excluded for any electric charge [12].

Before finishing this section, we comment on the electric charge of the B ball. This should be below the maximal electric charge [16] and negligible with respect to the baryon number. However, there is no symmetry to forbid the B ball to have an electric charge. For example, in a flat direction of Eq. (8), zero electric charge means that the field values of $\bar{u}_1$, $\bar{d}_1$, and $\bar{d}_2$ are equal to each other. However, this equality might be violated by SUSY breaking and the B ball may have a non-zero electric charge. In order to determine it, we also need to know the details of the scalar potential.

3 Evaporation of the B ball by the baryon-number-violating operators

In next section we will evaluate the evaporation rate of the B ball by the baryon-number-violating operators, using a technique described by Cohen *et al.* [17]. However, this technique is not applicable to cases including scattering, annihilation, or decays of the fermions bounded inside the Q ball. The energy release in the evaporation per unit charge is ω. This means that we cannot evaluate the evaporation rate for $\omega \lesssim 100$ MeV, where no mesons can be emitted from the B ball. Here, we discuss what may happen for both cases, $\omega \gtrsim 100$ MeV and $\omega \lesssim 100$ MeV, while we will evaluate the evaporation rate only for $\omega \gtrsim 100$ MeV in the next section.

We assume the SUSY SM with the R parity conservation. Then the baryon-number-violating operators are given by F terms of the effective operator with dimension larger than 5 or D terms with dimension larger than 6. The lowest baryon-number-violating operators in the F terms are given as

$$\mathcal{L} = \frac{1}{M_5} Q_i Q_j Q_k L_l|_{\theta^2} + \frac{1}{M_5'} \bar{u}_i \bar{e}_j \bar{u}_k \bar{d}_l|_{\theta^2} + \text{h.c.}, \tag{18}$$

where i, j, k, l are for the generations ($i \neq k$). These interactions change the charges of the B ball by $\Delta(B-L) = 0$ and $\Delta(B+L) = -2$.

Let us discuss typical examples. First, we assume that the B ball is composed of the flat direction in Eq. (8), $\bar{u}_2 \bar{d}_1 \bar{d}_2$. Inserting Eq. (8) in the above operators, we get the interaction[2]

$$\tfrac{1}{3M_5'} \phi^{\star 2} \bar{u}_1 \bar{e}_1. \tag{19}$$

Then, the final state is $(\pi^- e^+)$ for one baryon number. Here, d_1 in the pion is supplied by the surface of the B ball. The production $(\pi^- e^+)$ is allowed from the kinematics if $\omega \gtrsim 210$ MeV, since the typical momentum for each parton is $\sim \frac{1}{3}\omega$. (This will be shown in the next section.)

Here, notice there are other interactions, such as

$$\tfrac{1}{3M_5'} \phi^{\star 2} \bar{u}_3 \bar{e}_3. \tag{20}$$

[2] Notice that we define that the charge of ϕ is positive.

Because of kinematics, the primary fermions in this interaction, $\bar{u}_3$ and e_3^+, cannot be emitted from the B ball. The primary fermions may be bounded on the surface or inside of the B ball for a while, and decay or annihilate into the lighter states. In fact, u_3 and e_3 behave as a massless particle inside the Q ball if the above operator (20) is negligible. In the conventional SUSY-GUT, the baryon-number-violating dimension-5 operators are proportional to the fermion masses [18]; this process may then be enhanced and dominate over the others. If this process dominates, the final state and the spectrum may be different from the one mentioned above. We need a technique to calculate the transition rate of the primary quark, bounded in the B ball, to lighter states in order to derive the evaporation rate of the B ball. Keeping this possibility in mind, we will continue our discussion.

If $\omega \lesssim 210$ MeV, all quarks are bounded inside or on the surface of the B ball. This situation is also similar to the case mentioned above, and we cannot evaluate the evaporation rate. The final states are expected to be (e^+, e^-, ν, $\bar{\nu}$, $\bar{\nu}$) or (γ's, ν, $\bar{\nu}$, $\bar{\nu}$).

Next, if the B ball is composed of the flat direction $\bar{u}_1\bar{e}_1\bar{u}_2\bar{d}_1$, the final states are ($\pi^0$, e^+, e^-) or (2 π^0) for $\omega \gtrsim 280$ MeV. On the other hand, (π^0, $\bar{\nu}$, ν) is also included in the final states for the B ball composed of $Q_1Q_1Q_2L_1$. The typical momentum of each fermion is $\omega/4$ (the momentum of the pion is double of this). These arguments are applicable to the other B balls. The exceptions are cases where the B ball consists of

$$\bar{u}\bar{u}\bar{u}\bar{d}\bar{d}\bar{d}\bar{e}, \qquad \bar{u}\bar{u}\bar{d}\bar{d}\bar{d}\bar{d}. \tag{21}$$

In these cases, the dimension-5 operators are not effective, since the interaction with $\Delta B = \pm 2$ is needed, and the dimension-7 operators with $\Delta B = 2$ may work well,

$$\mathcal{L} = \frac{1}{M_7^3}\bar{u}_i\bar{u}_j\bar{d}_k\bar{d}_1\bar{d}_2\bar{d}_3, \tag{22}$$

where $i \neq j$. The final states are ($2\pi^0$, e^-), (π^+, π^-, e^-) for the former in Eq. (21), and ($2\pi^0$), (π^+, π^-) for the latter if the kinematics allows the processes.

Finally, we comment on the baryon-number-violating operators in the D terms. The lowest ones are

$$\mathcal{L} \;=\; \frac{1}{M_6^2}\bar{d}^\dagger\bar{u}^\dagger QL|_{\theta^2\bar{\theta}^2} + \frac{1}{M_6'^2}\bar{u}^\dagger\bar{e}^\dagger QQ|_{\theta^2\bar{\theta}^2}. \tag{23}$$

Since the relevant terms in the D-term operators have a derivative of the scalar, the evaporation rate is suppressed by ω/M_6, with respect to the F-term operators.

4 Evaporation rate of the B ball

In this section we present the evaporation rate of the B ball obtained by the baryon-number-violating operators. The technique to calculate it was developed by Cohen *et al.* [17]. They evaluate the evaporation rate of the L ball to neutrinos by the lepton-number-conserving interaction. The evaporation process to neutrinos is equivalent to the neutrino pair production on the L ball background. They construct a quantum field theory preserving a symmetry on the L ball background, a simultaneous time translation and L phase rotation, and derive the evaporation rate through the Bogoliubov transformation between the creation and annihilation operators in the asymptotic fields of neutrino at $t \to \pm\infty$. The result is given by the transition amplitude to the outgoing anti-neutrino from the incoming neutrino.

We generalize their result and apply it to the B ball evaporation. In our case the interactions to create the fermion pairs are baryon-number-violating. However, we may use the formula as the zeroth order of the Yukawa coupling constants. Also, if the interactions are the dimension-5 operators, they preserve $(B-L)$. Then, when the B ball is composed of $\bar{u}\bar{d}\bar{d}$, we can use their result by regarding the B ball as the (B$-$L) ball. In this section, we first show the properties of the Q ball evaporation process. After that, we present the evaporation rate of the B ball and compare it with the age of the Universe.

Since the generalization of the technique developed by Cohen is straight-forward, we summarize the result without repeating their calculation here.[3] The Yukawa interaction contributing to the evaporation is

$$\mathcal{L} = \phi\psi_1\psi_2 \tag{24}$$

where ϕ is replaced by the Q ball background. The global $\mathrm{U}_Q(1)$ charge for the scalar ϕ is 1, while those for fermions, ψ_1 and ψ_2, are p and $(-p-1)$, respectively. This $\mathrm{U}_Q(1)$ symmetry stabilizes of the Q ball. When adopting the thin-wall approximation for the Q

[3] Eq. (3.4) in Ref. [17] has a typo. The second term in the bracket has wrong signs.

ball background, ϕ is taken as

$$\phi \;=\; \begin{cases} v\ \mathrm{e}^{-i\omega t} & (r \le R_Q), \\ 0 & (r > R_Q). \end{cases} \tag{25}$$

In this set-up, the evaporation rate of the Q ball is given to be

$$\frac{dQ}{dt} \;=\; \sum_{j=1/2}^{\infty} \int_0^{\omega} \frac{dk}{4\pi} (2j+1) |T(k,j)|^2, \tag{26}$$

where k and j are the energy and the total orbit momentum for the fermion. The explicit form of the transition amplitude $T(k,j)$ is given to be

$$\begin{aligned} T(k,j)^{-1} \;=&\; \frac{w_0 - k}{vk} \frac{(h^{(1)}_{++} j_{--} - h^{(1)}_{-+} j_{+-})(h^{(2)}_{+-} j_{-+} - h^{(2)}_{--} j_{++}) w'_-}{(h^{(1)}_{++} h^{(2)}_{-+} - h^{(1)}_{-+} h^{(2)}_{++})(j_{-+} j_{+-} - j_{--} j_{++})} \\ &- \frac{w_0 - k}{vk} \frac{(h^{(1)}_{++} j_{-+} - h^{(1)}_{-+} j_{++})(h^{(2)}_{+-} j_{--} - h^{(2)}_{--} j_{+-}) w'_+}{(h^{(1)}_{++} h^{(2)}_{-+} - h^{(1)}_{-+} h^{(2)}_{++})(j_{-+} j_{+-} - j_{--} j_{++})}. \end{aligned} \tag{27}$$

The transition amplitude is calculated assuming that ψ_1 and ψ_2 are massless. Here,

$$\begin{aligned} h^{(i)}_{\pm +} &= h^{(i)}_{j \pm \frac{1}{2}}(k R_Q) \qquad (i = 1, 2), \\ h^{(i)}_{\pm -} &= h^{(i)}_{j \pm \frac{1}{2}}((\omega - k) R_Q) \qquad (i = 1, 2), \\ j_{\pm +} &= j_{j \pm \frac{1}{2}}(k_+ R_Q), \\ j_{\pm -} &= j_{j \pm \frac{1}{2}}(k_- R_Q), \\ w'_{\pm} &= k + k_{\pm} - \omega, \end{aligned} \tag{28}$$

with $k_\pm = \omega/2 \pm \sqrt{(k - \omega/2)^2 - v^2}$. The functions, $h^{(i)}_j(x)$ $(i = 1, 2)$ and $j_j(x)$, are the Hankel and Bessel functions. The amplitude $T(k,j)$ has following properties:

i) $T(0, j) = T(\omega, j) = 0$,

ii) $T(k, j) = T(\omega - k, j)$,

iii) $T(k, j)$ is independent of the fermion charge p.

Also, if R_Q is not so large with respect to ω^{-1}, the contributions from the higher j modes dump quickly, and the numerical calculation is not so difficult.[4]

[4] In Ref. [19] the evaporation rate of the Q ball with finite R_Q is calculated.

In Fig. 2 we show the evaporation rate of the Q ball, dQ/dt, for $R_Q\omega = 1$ and 10 as a function of v/ω. Here, the evaporation rate is normalized by the maximum value,

$$\left(\frac{dQ}{dt}\right)_{\rm Max} = \frac{\omega^3 R_Q^2}{48\pi}. \tag{29}$$

The qualitative behaviour of the evaporation rate is easy to understand. When $v/\omega > 1$, the fermion pairs are produced only on the surface of the Q ball, since the production inside the Q ball is suppressed by the Pauli blocking. Then, the evaporation rate is bounded by the maximum outgoing flux of the fermion pair with the total energy ω, and the maximum evaporation rate is derived as in Eq. (29) [17].

On the other hand, if $v/\omega < 1$, the fermion pair production from the outer shell of the Q ball, whose width is $\sim 1/v$, contributes to the evaporation. This is because the penetration length of the fermion inside the Q ball, $\sim 1/v$, is larger than $1/\omega$. Roughly speaking, regarding the decay rate of a quantum with unit charge ω, the evaporation rate is $\sim \omega \times (\omega v^2) \times (R_Q^2/v) = v\omega^2 R_Q^2$, and it is suppressed by v/ω compared with $(dQ/dt)_{\rm Max}$. Here, ωv^2 is the charge density inside the Q ball. This can be proved explicitly in the limit of a large R_Q [17]. In this limit, the evaporation rate becomes

$$\frac{dQ}{dt} = \frac{\omega^2 v R_Q^2}{16}. \tag{30}$$

This behaviour is not valid for $1/v \gtrsim R_Q$. In this case, the whole region inside the Q ball contributes to the evaporation, and then the evaporation rate behaves, as $\sim v^2\omega^2 R_Q^3$ as in Fig. 2.

The above qualitative behaviour can be seen in the energy spectrum of the fermion in the evaporation. In Fig. 3 we show the fermion energy spectrum for $v/\omega = 10$, 10^{-1}, 10^{-3}, 10^{-5}, the in cases $R_Q\omega = 1$ and 10. The spectra for $v/\omega = 10$ are almost independent of $R_Q\omega$. On the other hand, the spectrum has a peak around $\omega/2$, and it becomes steeper for smaller v and larger R_Q.

Now we have prepared for calculating the evaporation rate of the B ball. Here, we use the parametrizations given in Eqs. (11) and (16) for the thin-wall approximation. This approximation may make an $O(1)$ error for the evaluation of the evaporation rate.

In order to make our discussion clear, we assume that the B ball is composed of the flat direction $\bar{u}_2\bar{d}_1\bar{d}_2$ (Eq. (8)), and that evaporates into $(\pi^- e^+)$ by the interaction in Eq. (19).

In this case, the ϕ, which is canonically normalized, has the baryon number $q = 1/3$, and Eq. (19) becomes

$$\mathcal{L} = \frac{\tilde{\phi}^2}{3M_5'} e^{i\frac{2}{3}\omega t} \bar{u}_1 \bar{e}_1 \tag{31}$$

inside the B ball. We can apply the above formula by inserting

$$v = \frac{\tilde{\phi}^2}{3M_5'} \tag{32}$$

and rescaling ω due to the charge definition. As mentioned in the last section, e_1^+ and $\bar{u}_1$ in the final state share $2\omega/3$ from this interaction. The d_1 in π^- is supplied from the surface, since d_1 is heavy with the gaugino inside the B ball. The d_1 shares $2\omega/3$ with the other d_1 in the final state. The time scale of the d_1 emission is of the order of $3\omega^{-1}/2$, and the effect on the evaporation rate is negligible.[5] Here we have to note that π^- is a pseudoscalar, and a chirality flip is required to create a π^- from d_1 and $\bar{u}_1$. The associated suppression F may be of the order of $(m_q/f_\pi)^2 \sim 10^{-3}$, where f_π is the pion decay constant, because it comes from the pion current interaction $J^\mu \partial_\mu \pi / f_\pi$. In this article we do not attempt to estimate this suppression factor precisely. We take $F = 1$ when we present our numerical result.

In Fig. 4 we show the evaporation time $(dQ/Qdt)^{-1}$ of the B ball composed of $\bar{u}_2\bar{d}_1\bar{d}_2$. The two solid lines are for the cases the B ball originates from the GMSB or supergravity scalar potentials. Here, for the supergravity B ball, we fix $m_{3/2} = 300$ MeV and $|K|^{-\frac{1}{2}} = 10$ and use Eq. (16) for ϕ, R_Q, and ω. Also, for the GMSB B ball, we use Eq. (11) with $m = 1$ TeV and $M = 10^2$ TeV. We plot the line of the GMSB B ball for $\omega > 210$ MeV. The suppression factor of the dimension-5 operator M_5' is taken to be 10^{30} GeV, which is completely beyond the constraint from the negative search in proton decay [20].

In this figure, the evaporation time of the supergravity B ball decreases as Q increases for $Q \lesssim 10^{34}$. This is because v is much smaller than ω and R_Q^{-1}, and v is proportional to Q. On the other hand, when $Q \gtrsim 10^{34}$, the evaporation time increases since (dQ/dt) is independent of v for $v/\omega > 1$. If the evaporation time is less than the age of the Universe ($t_0 \simeq 10^{10}$years), the B ball cannot survive to this day. In this figure we take

[5] The emission of d_1 is similar to the case of $v/\omega > 1$ in Fig. 2; the emission rate is understood from the analogy.

$m_{3/2} = 300$ MeV. For smaller $m_{3/2}$, beyond the validity of our calculation, if the qualitative nature does not change drastically, $(dQ/Qdt)^{-1}$ may become larger by $1/m_{3/2}^3$ when $Q \lesssim 10^{33}(m_{3/2}/1\ \text{GeV})^{-1}$ and $1/m_{3/2}$ when $Q \gtrsim 10^{33}(m_{3/2}/1\ \text{GeV})^{-1}$. The evaporation time of the GMSB B ball in this figure is proportional to $Q^{-\frac{1}{4}}$. This is because $v \ll \omega$ and v is proportional to $Q^{\frac{1}{2}}$, not Q as the supergravity B ball.

In Fig. 5 we show the evaporation time of the B ball composed of $\bar{u}_2\bar{d}_1\bar{d}_2$ as a function of Q and M_5', in a case where the B ball originates from the supergravity scalar potential, with $m_{3/2} = 300$ MeV and $|K|^{-\frac{1}{2}} = 10$. The thin lines are for $(dQ/Qdt)^{-1} = 10^0$, 10^{20}, 10^{40} years. The bold lines are for the age of the Universe (10^{10} years) and the big-bang nucleosynthesis time (1 second). For $Q \gtrsim 10^{38-40}$, $\tilde{\phi}_0$ is larger than the Planck mass, and the region may be disfavoured from the theoretical point of view. The region for $Q \lesssim 10^{23}$ is an unphysical region, since the B ball should be an unstable GMSB B ball from Fig. 1. This means that M_5' should be larger than 10^{28} GeV at least so that the B ball behaves as the DM of the Universe when $m_{3/2} = 300$ MeV.

If the B ball evaporates before the time of the big-bang nucleosynthesis, it has no effect on the cosmology, except for the dilution of the baryon number of the Universe. On the other hand, if the B ball evaporation occurs after the nucleosynthesis and the abundance is not negligible, the energetic particles in the final state may destroy the success of the big-bang nucleosynthesis. Also, the entropy production may change the expansion rate of the Universe. In this article, we do not discuss the AD baryogenesis in detail; however, the evaporation of the B ball by the baryon-number-violating operators may give a constraint in the AD baryogenesis on the GMSB model, which predicts a B ball with large Q.

Finally, we comment on the other B balls. If the B ball is composed of $\bar{u}_1\bar{d}_1\bar{d}_2$, the fermions $\bar{u}_1$, $\bar{d}_1$, and $\bar{d}_2$ are massive inside the B ball, and this might be in conflict with the assumption in the above formula, Eq. (27). However, the fermion associated with the flat direction, which is a linear combination of $\bar{u}_1$, $\bar{d}_1$ and $\bar{d}_2$, is still massless on the flat direction condensation, and the above formula is thus still applicable.

5 Constraint from observation of the cosmic rays

Even if some relic particle has a lifetime longer than the age of the Universe, the decay products may distort the cosmic-ray background. This leads to a constraint on the decaying DM. In fact, the relic axion [21] and the relic Kaluza-Klein graviton [22] are constrained from the the cosmic diffused gamma ray. In this section we derive constraints on the B ball evaporation rate from the cosmic diffused gamma background and the cosmic ray position flux.

First, we start from the position flux induced by the B ball evaporation. The positrons in the evaporation of the B ball have an almost monochromatic energy spectrum if the positron is the primary fermion in the evaporation process and if $R_Q\omega \gtrsim 1$ and $v/\omega \ll 1$, as discussed in the previous section. However, the positrons are diffused by the galactic magnetic field and lose their energy through the inverse Compton and the synchrotron processes, by the starlight and the cosmic microwave background. In this article, we consider the standard diffusion model for the propagation of positrons in the galaxy, which was summarized in Ref. [23]. In that article, the positron flux from the neutralino annihilation in the Halo was calculated, assuming that the neutralino is the DM in the Universe.

In their formulae, the diffusion zone of the positron in our galaxy is a slab of the thickness $2L \simeq 6$kpc, and the positron density becomes zero outside that region, since the positrons escape freely there. The standard diffusion-loss equation for the positron density spectrum (dn_{e^+}/dE) is

$$\frac{\partial}{\partial t}\frac{dn_{e^+}}{d\epsilon} = \overrightarrow{\nabla}\cdot\left[K(\epsilon,\mathbf{x})\overrightarrow{\nabla}\frac{dn_{e^+}}{d\epsilon}\right] + \frac{\partial}{\partial\epsilon}\left[b(\epsilon,\mathbf{x})\frac{dn_{e^+}}{d\epsilon}\right] + \frac{dn_{e^+}^{(0)}}{dtd\epsilon}, \tag{33}$$

where $\epsilon = E/(1\text{ GeV})$. Here, $K(\epsilon,\mathbf{x})$ is the diffusion constant, $b(\epsilon,\mathbf{x})$ the positron energy loss rate, and $(dn_{e^+}^{(0)}/dtd\epsilon)$ the source term.

In the diffusion zone the diffusion constant $K(\epsilon)$ is

$$\begin{aligned} K(\epsilon) &= K_0(C+\epsilon^\alpha) \\ &\simeq 3\times 10^{27}\left(3^{0.6}+\epsilon^{0.6}\right)\ \text{cm}^2\ \text{s}^{-1} \end{aligned} \tag{34}$$

for $E \lesssim 3$ GeV, and the positron energy loss rate $b(\epsilon)$ is

$$\begin{aligned} b(\epsilon) &= \frac{1}{\tau_E}\epsilon^2 \\ &\simeq 10^{-16}\epsilon^2 \text{ s}^{-1}. \end{aligned} \tag{35}$$

By deriving the stable solution for the diffusion-loss equation in the above environment, the positron spectrum originated from the DM is given as

$$\frac{dn_{e^+}}{d\epsilon} = \epsilon^{-2}\int_{\epsilon}^{\infty} d\epsilon' \frac{dn_{e^+}^{(0)}(\epsilon')}{dtd\epsilon'}\tau_D(\epsilon,\epsilon'). \tag{36}$$

Here, the energy-dependent diffusion time $\tau_D(\epsilon,\epsilon')$ is

$$\begin{aligned} \tau_D(\epsilon,\epsilon') &= \frac{1}{4K_0\Delta v}\sum_{n=-\infty}^{+\infty}\sum_{\pm}\mathrm{Erf}\left(\frac{(-)^n L \pm 2nL \mp z}{\sqrt{4K_0\tau_E\Delta v}}\right) \\ &\quad \times \int_0^{\infty} dr' r' f(r')\tilde{I}_0\left(\frac{2rr'}{4K_0\tau_E\Delta v}\right)\mathrm{e}^{-\frac{(r-r')^2}{4K_0\tau_E\Delta v}} \end{aligned} \tag{37}$$

where r and z are cylindric coordinates for the position of the solar system in our galaxy ($r = 8.5$ kpc and $z = 0$). The function $\tilde{I}_0(x)$ is $I_0(x)\mathrm{e}^{-x}$ with $I_0(x)$ the modified Bessel function, and $\mathrm{Erf}(x)$ is the error function. We neglect the energy-dependent part of the diffusion constant, and

$$\Delta v \equiv C\left(\frac{1}{\epsilon} - \frac{1}{\epsilon'}\right). \tag{38}$$

The function $f(r)$ is

$$f(r) \equiv \int_{-L}^{L} dz = g_{\mathrm{DM}}^m(\sqrt{r^2+z^2}), \tag{39}$$

with $g_{\mathrm{DM}}(r_{sph})$ ($r_{sph}^2 = r^2 + z^2$) the DM density profile. The exponent m is 1 for the decay process of the DM, and 2 for the annihilation process. In this article, we use the isothermal distribution for the DM density profiles,

$$g_{\mathrm{DM}}(r_{sph}) = \frac{a^2}{r_{sph}^2 + a^2}, \tag{40}$$

with $a = 5$ kpc. The N-body simulation suggests the cuspy density profile at the centre of the galaxy [24], and it may not be consistent with the isothermal distribution. However, the decay process is not sensitive to the density profile, and we thus use the isothermal distribution for the DM here.

If the positron flux comes from the evaporation of the B ball by the baryon-number-violating dimension-5 operators, the source term $(dn_{e^+}^{(0)}/dtdE)$ is

$$\frac{dn_{e^+}^{(0)}}{dtdE} = n_0 \frac{dQ}{dt}\delta(E - q\omega). \qquad (41)$$

Here, we simplify the spectrum of the positron as a monochromatic one. This is justified for $R_Q\omega > 1$ and $v \ll \omega$ giving a long evaporation time, as shown in Fig. 3. We take the number density of the B ball n_0 as $Q\omega_0 n_0 = 0.3$ GeV cm^{-3}. The diffusion and the energy reduction in the propagation makes a tail below $q\omega$ in the positron spectrum. In Fig. 6 we show the primary positron flux spectrum $(d\Phi_{e^+}^{(p)}/dE)$, which is given as $(d\Phi_{e^+}^{(p)}/dE) \equiv (c/4\pi)(dn_{e^+}/dE)$, assuming $q\omega = 300$ MeV, $q = 1/3$, and $(dQ/Qdt)^{-1} = 10^{18}$ years. Also, we take $\omega_0 = \omega$ as for the supergravity B ball. If $\omega_0 = 4\omega/3$ as for the GMSB B ball, the primary flux is reduced by 3/4.

While the cosmic ray positron flux is measured for an energy larger than about 70 MeV [25], the theoretical estimate of the background has uncertainties. The secondary positron flux, which comes from the nuclear interaction of the primary cosmic rays in the interstellar space, is estimated in Ref. [26]. The result is fitted in Ref. [23] as

$$\frac{d\Phi_{e^+}^{(s)}}{dE} = \frac{4.5\epsilon^{0.7}}{1 + 650\epsilon^{2.3} + 1500\epsilon^{4.2}} \text{ cm}^{-2}\text{ s}^{-1}\text{ sr}^{-1}\text{ GeV}^{-1}. \qquad (42)$$

The qualitative behaviour of the positron fraction $(e^+/(e^+ + e^-))$ in the cosmic ray, increasing of the positron flux at lower energy, is realized by assuming that the positron is of a secondary origin. However, the effect of the solar modulation from the solar wind and the magnetosphere to both the positron and electron fluxes is larger at lower energy. Especially, the introduction of the charge-dependent solar modulation makes the fit to the observation worse [23]. Therefore, we derive a conservative constraint on the evaporation time of the B ball by imposing a condition that the peak of the primary flux from the B ball be smaller than ten times of the secondary flux, Eq. (42), and we obtain

$$\left(\frac{dQ}{Qdt}\right)^{-1} \gtrsim 2\, q \times 10^{19} \text{ years} \left(\frac{Q\omega_0 n_0}{0.3 \text{ GeV cm}^{-3}}\right)\left(\frac{q\omega}{100\text{MeV}}\right)^{-1}, \qquad (43)$$

for $q\omega \sim 100$ MeV. From Fig. 5, this constraint means that M_5' should be larger than 10^{32} GeV for $Q \gtrsim 10^{22}$, assuming the B ball is the DM of the Universe and $m_{3/2} = 300$ MeV.

Next, let us consider the distortion of the cosmic background radiation by π^0 from the B ball evaporation. Although the gamma, which comes from $\pi^0 \to 2\gamma$, is almost monotonic at production time, the energy is reduced by the red-shift. As a result, the energy spectrum of the gamma from the B ball evaporation is

$$\frac{dn_\gamma}{dE} = 3n_0 \frac{dQ}{dt} t_0 E^{\frac{1}{2}} (q\omega)^{-\frac{3}{2}}, \tag{44}$$

for $E < q\omega$, assuming $(dQ/Qdt)^{-1} \gg t_0$. Here, we assume that the B ball evaporates through the baryon-number-violating dimension-5 operators and that the π^0 has an energy $2q\omega$. From this equation (44), the flux of gamma rays for $E < q\omega$ is

$$\begin{aligned} \frac{d\Phi_\gamma}{dE} &= 7.9\, h^2 \times 10^6 \ \ \mathrm{cm}^{-2}\ \mathrm{s}^{-1}\ \mathrm{sr}^{-1}\ \mathrm{GeV}^{-1} \\ &\quad \times \left(\frac{t_0}{(dQ/Qdt)^{-1}}\right)\left(\frac{Q\omega_0 n_0}{\rho_C}\right)\left(\frac{\omega_0}{0.1\ \mathrm{GeV}}\right)^{-1}\left(\frac{q\omega}{0.1\ \mathrm{GeV}}\right)^{-\frac{3}{2}}\left(\frac{E}{0.1\ \mathrm{GeV}}\right)^{\frac{1}{2}}. \end{aligned} \tag{45}$$

Here, ρ_C is the critical density of the Universe ($\rho_C = 1.1h^2 \times 10^{-5}$ GeV cm^{-3}). In Fig. 7 we show the spectrum of the gamma rays flux from the B ball evaporation ($d\Phi_\gamma/dE$), assuming $q\omega = 250$ MeV, $q = 1/4$, and 10^{19} years for the evaporation time $(dQ/Qdt)^{-1}$. Here we fix $h = 0.7$ and $t_0 = 10^{10}$ years. Also, we take $\omega_0 = \omega$ as for the supergravity B ball.

EGRET determines the extragalactic gamma ray background spectrum between 0.1 and ~ 50 GeV [27] as

$$\frac{d\Phi_\gamma}{dE} = (7.32 \pm 0.34) \times 10^{-6} \left(\frac{E}{0.451\mathrm{GeV}}\right)^{-2.10\pm0.03} \ \mathrm{cm}^{-2}\ \mathrm{s}^{-1}\ \mathrm{sr}^{-1}\ \mathrm{GeV}^{-1}. \tag{46}$$

Here, imposing the condition that the peak of the gamma spectrum from the B ball be smaller than Eq. (46) leads us to a constraint on the evaporation time of the B ball:

$$\left(\frac{dQ}{Qdt}\right)^{-1} \gtrsim 5\, qh^2 \times 10^{20}\ \mathrm{years} \left(\frac{t_0}{10^{10}\ \mathrm{years}}\right)\left(\frac{Q\omega_0 n_0}{\rho_C}\right)\left(\frac{q\omega}{100\mathrm{MeV}}\right)^{0.1}, \tag{47}$$

for $q\omega \sim 100$ MeV. This is one order of magnitude stronger than the constraint from the positron flux.

6 Conclusions and discussion

In this article we discuss the stability of the B ball in the GMSB model. The B ball is predicted to exist in the GMSB model, assuming AD baryogenesis. While the stability of the B ball comes from the baryon-number conservation, the baryon-number-violating interaction is required to make the baryonic AD condensation, which is a seed for the B ball. The B ball could therefore be unstable. We find that a larger B ball evaporates faster, since the field value inside the B ball enhances the evaporation rate.

The evaluation of the evaporation rate of the B ball suffers from various difficulties, and we therefore restrict our calculation to a B ball of the mass-to-charge ratio $\omega_0 \gtrsim 100$ MeV. We derive the constraints on the B ball charge and the interactions, when the B ball is composed of $\bar{u}_2\bar{d}_1\bar{d}_2$, as an example. Neglecting the chiral suppression from the final state, the suppression factor of the baryon-number-violating dimension-5 operator M_5' should be larger than $10^{27}(Q/10^{20})^{\frac{1}{2}}$ GeV for $m_{3/2} = 300$ MeV, so that the evaporation time $(dQ/Qdt)^{-1}$ is longer than the age of the Universe ($t_0 \simeq 10^{10}$ years). The final states of the evaporation may include the almost monochromatic positron or π^0. If the B ball is the DM of the Universe, the evaporation may give a contribution to the extragalactic gamma ray background spectrum and to the cosmic ray positron flux. From the current data, we give constraints on the evaporation time from the primary positron flux and the gamma ray background, for $\omega_0 \sim 100$ MeV, of $(dQ/Qdt)^{-1} \gtrsim 10^{18}$ or 10^{19} years, which are stronger than the constraint from the age of the Universe.

The instability of the B ball will have some impact on the cosmology of the GMSB model. In this article, we do not discuss detail of the AD baryogenesis. The existence of the B ball may be preferred, as far as the AD field with the baryon numbers condensates in the GMSB model. If the B ball has an evaporation time shorter than the age of the Universe, the evaporation may supply the entropy production and the injection of a high-energy positron after the big-bang nucleosynthesis. Note that the B ball may explain the reionization of the Universe, indicated by the Gunn-Peterson test [28]. It is well-known that the Universe is ionized at $z \sim 3$, from the absence of the strong Layman-alpha scattering light. While this may be explained by the huge star formation at the time, it may come from the late-time decay of an exotic relic particle, and the B ball may work for it.

Acknowledgements

We would like to thank S. Asai, G. Giudice, S. Kasuya, M. Kawasaki, L. Roszkowski, and N. Sugiyama for useful discussions. This work was started at the visiting program at the YITP of the Kyoto University. This was also supported in part by the Grant-in-Aid for Scientific Research from the Ministry of Education, Science, Sports and Culture of Japan, on Priority Area 707 "Supersymmetry and Unified Theory of Elementary Particles" (J.H.) and Grant-in-Aid for Scientific Research from the Ministry of Education (12047217, M.M.N).

References

[1] For a review, see G. F. Giudice and R. Rattazzi, Phys. Rep. **322** (1999) 419 [hep-ph/9801271].

[2] M. Dine, A. E. Nelson, Y. Nir and Y. Shirman, Phys. Rev. D **53** (1996) 2658 [hep-ph/9507378].

[3] H. Pagels and J. R. Primack, Phys. Rev. Lett. **48** (1982) 223;
T. Moroi, H. Murayama and M. Yamaguchi, Phys. Lett. **B303** (1993) 289.

[4] K. I. Izawa, Y. Nomura, K. Tobe and T. Yanagida, Phys. Rev. D **56** (1997) 2886 [hep-ph/9705228].

[5] I. Affleck and M. Dine, Nucl. Phys. **B249** (1985) 361.

[6] A. de Gouvea, T. Moroi and H. Murayama, Phys. Rev. D **56** (1997) 1281 [hep-ph/9701244].

[7] A. Kusenko and M. Shaposhnikov, Phys. Lett. **B418** (1998) 46 [hep-ph/9709492].

[8] S. Coleman, Nucl. Phys. **B262** (1985) 263.

[9] A. Kusenko, Phys. Lett. **B405** (1997) 108 [hep-ph/9704273].

[10] K. Enqvist and J. McDonald, Nucl. Phys. **B570** (2000) 407 [hep-ph/9908316];
S. Kasuya and M. Kawasaki, Phys. Rev. D **61** (2000) 041301 [hep-ph/9909509]; Phys. Rev. D **62** (2000) 023512 [hep-ph/0002285].

[11] A. Kusenko, V. Kuzmin, M. Shaposhnikov and P. G. Tinyakov, Phys. Rev. Lett. **80** (1998) 3185 [hep-ph/9712212].

[12] J. Arafune, T. Yoshida, S. Nakamura and K. Ogure, Phys. Rev. D **62** (2000) 105013 [hep-ph/0005103].

[13] S. Kasuya and M. Kawasaki, Phys. Rev. Lett. **85** (2000) 2677 [hep-ph/0006128].

[14] M. Dine, L. Randall and S. Thomas, Nucl. Phys. **B458** (1996) 291 [hep-ph/9507453].

[15] K. Enqvist and J. McDonald, Phys. Lett. **B425** (1998) 309 [hep-ph/9711514]; Nucl. Phys. **B538** (1999) 321 [hep-ph/9803380]; Phys. Lett. **B440** (1998) 59 [hep-ph/9807269].

[16] K. Lee, J. A. Stein-Schabes, R. Watkins and L. M. Widrow, Phys. Rev. D **39** (1989) 1665.

[17] A. Cohen, S. Coleman, H. Georgi and A. Manohar, Nucl. Phys. **B272** (1986) 301.

[18] N. Sakai and T. Yanagida, Nucl. Phys. **B197** (1982) 533;
S. Weinberg, Phys. Rev. D **26** (1982) 287;
P. Nath, A. H. Chamseddine and R. Arnowitt, Phys. Rev. D **32** (1985) 2348;
J. Hisano, H. Murayama and T. Yanagida, Nucl. Phys. **B402** (1993) 46 [hep-ph/9207279].

[19] T. Multamaki and I. Vilja, Nucl. Phys. **B574** (2000) 130 [hep-ph/9908446].

[20] T. Goto and T. Nihei, Phys. Rev. D **59** (1999) 115009 [hep-ph/9808255].

[21] M. S. Turner, Phys. Rev. Lett. **59** (1987) 2489.

[22] L. J. Hall and D. Smith, Phys. Rev. D **60** (1999) 085008 [hep-ph/9904267].

[23] E. A. Baltz and J. Edsjo, Phys. Rev. D **59** (1999) 023511 [astro-ph/9808243].

[24] J.F. Navarro, C.S. Frenk and S.D.M. Whilte, Astrophys. J. **490** (1997) 493;
J. Dubinski and R.G. Carlberg, Astrophys. J. **378** (1991) 496;
S.W. Warren *et al.*, Astrophys. J. **399** (1992) 405.

[25] See references in S. Coutu *et al.*, Astropart. Phys. **11** (1999) 429;
also, see references in [23].

[26] I.V. Moskalenko and A.W. Strong, Astrophys. J. **493** (1998) 694 .

[27] P. Sreekumar *et al.*, Astrophys. J. **494** (1998) 523;
also, see F.W. Stecker and M.H. Salamon, Proc. 26th ICRC, Vol. 3, p. 313 [astro-ph/9909157].

[28] J.E. Gunn and B.A. Peterson, Astrophys. J. **142** (1965) 1633.

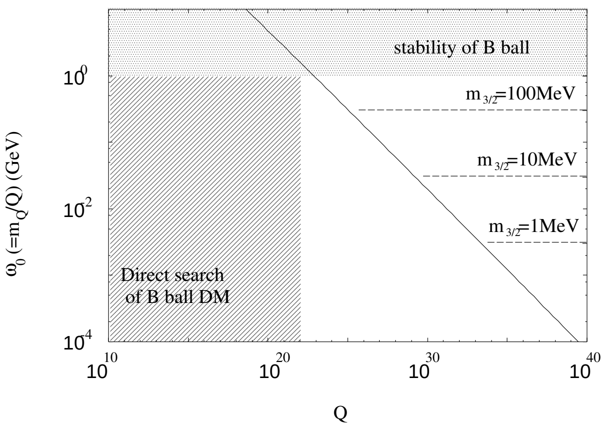

Figure 1: The mass-to-charge ratio of the B ball in the GMSB model. The horizontal axis is for the baryon number. The solid line is for the B ball, which comes from the flat-direction potential of the GMSB model. The dashed lines are for those from the supergravity contribution to the potential ($m_{3/2} = 10^{-1}$, 10^{-2}, and 10^{-3} GeV). Here, we take the SUSY breaking scale in the SUSY SM $m = 1$ TeV and the messenger scale $M = 10^2$ TeV. In the region above 1 GeV the B ball is unstable. The region for $Q < 10^{22}$ is excluded by the direct search for the B ball dark matter.

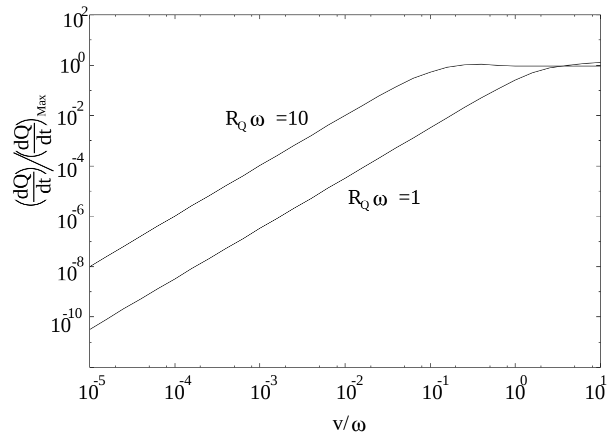

Figure 2: The Q ball evaporation rate for $R_Q\omega = 1$ and 10 as a function of v/ω. Here, the evaporation rate is normalized by the maximum value $(dQ/dt)_{\rm Max}$. (See Eq. (29) for the definition.) In this calculation we adopt the thin-wall approximation as in Eq. (25).

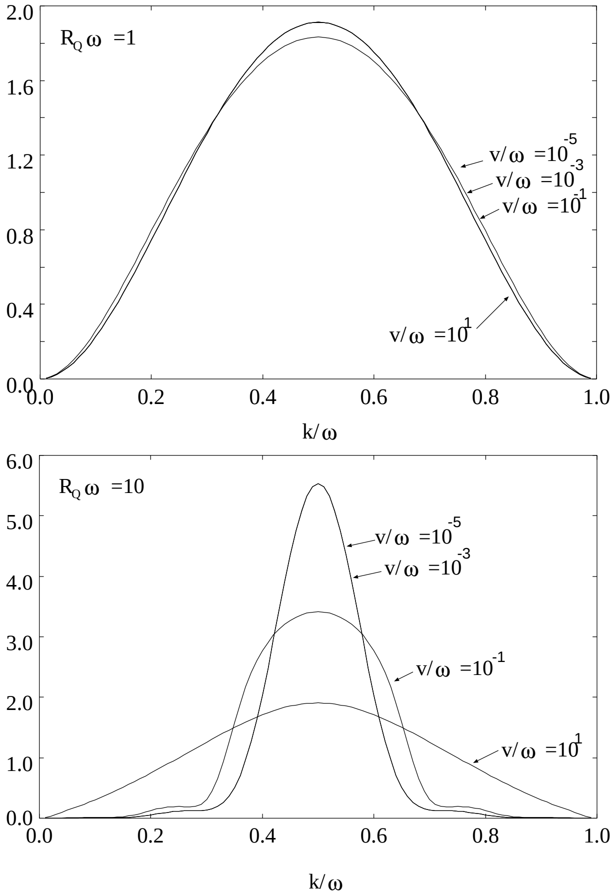

Figure 3: The energy spectrum of the fermion in the evaporation when $R_Q\omega = 1$ and 10. Here we take $v/\omega = 10$, 10^{-1}, 10^{-3}, 10^{-5}. In this calculation we adopt the thin-wall approximation as in Eq. (25).

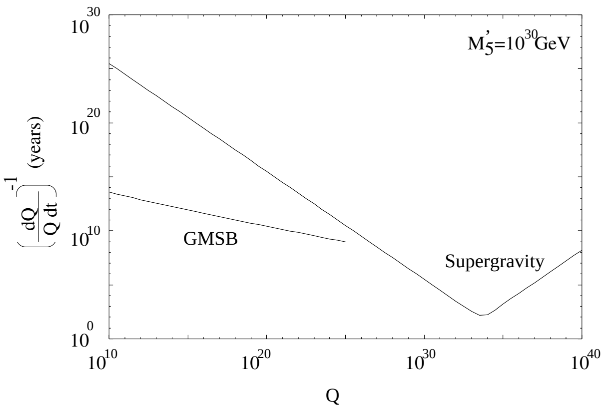

Figure 4: The evaporation time $(dQ/Qdt)^{-1}$ of the B ball composed of $\bar{u}_2\bar{d}_1\bar{d}_2$. The two solid lines are for the cases the B ball originates from the GMSB or supergravity scalar potentials. We take $m = 1$ TeV and $M = 10^2$ TeV for the GMSB B ball line and $m_{3/2} = 300$ MeV for the supergravity B ball line. For the other parameters for the B ball configuration, see the text. We plot the lines for $\omega > 210$ MeV. The suppression factor of the dimension-5 operator M_5' is taken to be 10^{30} GeV.

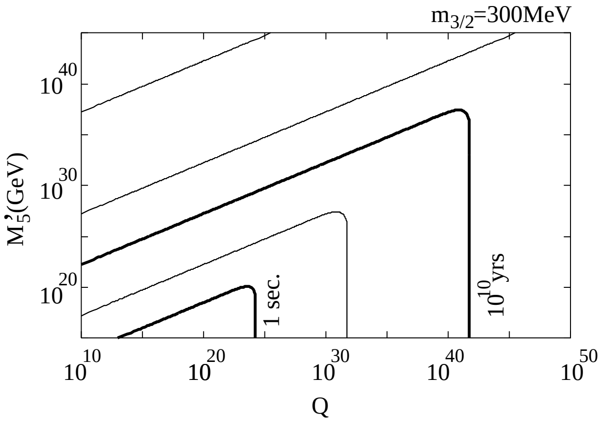

Figure 5: The evaporation time $(dQ/Qdt)^{-1}$ of the B ball composed of $\bar{u}_2\bar{d}_1\bar{d}_2$ as a function of Q and M_5', in the case where the B ball originates from the supergravity scalar potential with $m_{3/2} = 300$ MeV and $|K|^{-\frac{1}{2}} = 10$. The thin lines are for $(dQ/Qdt)^{-1} = 10^0$, 10^{20}, 10^{40} years, and the bold lines are for $(dQ/Qdt)^{-1} = 10^{10}$ years and 1 second.

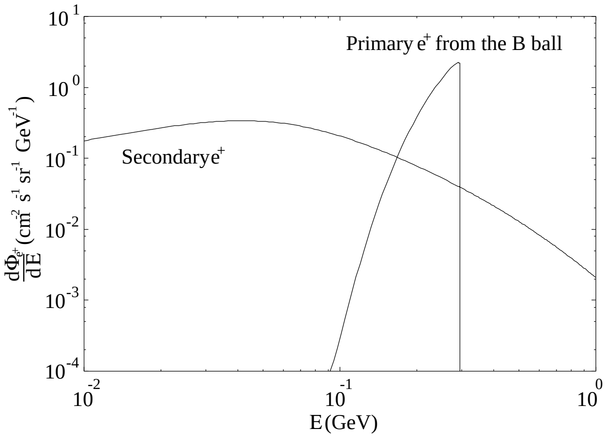

Figure 6: The primary and secondary positron flux spectra $d\Phi_{e^+}/dE$. The primary flux comes from the evaporation of the B ball, assuming $q\omega = 300$ MeV, $q = 1/3$, $\omega = \omega_0$, as for the supergravity B ball, and an evaporation time $(dQ/Qdt)^{-1} = 10^{18}$ years. The number density is fixed by $Q\omega_0 n_0 = 0.3$ GeV cm^{-3}. The line for the secondary positron flux is given in Ref. [23].

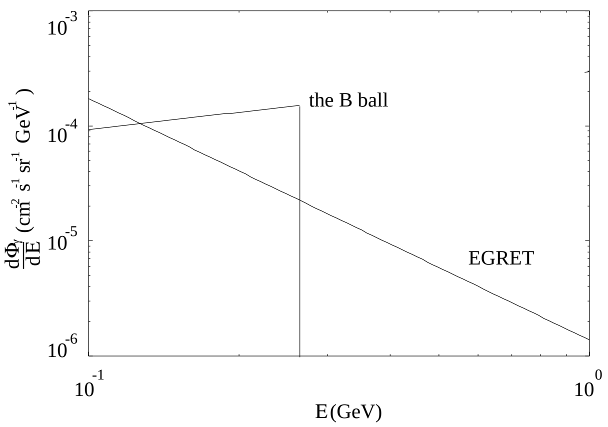

Figure 7: The spectrum of the gamma flux from the B ball evaporation $(d\Phi_\gamma/dE)$, assuming $q\omega = 250$ MeV, $q = 1/4$, $\omega = \omega_0$, and $(dQ/Qdt)^{-1} = 10^{19}$ years. The number density is fixed as $Q\omega_0 n_0 = \rho_C$ with $h = 0.7$. The result from EGRET is also shown.